Sensors and Actuators A 299 (2019) 111579

Contents lists available at ScienceDirect

Sensors and Actuators A: Physical

journal homepage: www.elsevier.com/locate/sna

A flexible capacitive sensor based on the electrospun PVDF nanofiber membrane with carbon nanotubes

Xiaofeng Yang [1], Yishou Wang [1], Xinlin Qing*

School of Aerospace Engineering, Xiamen University, Xiamen, 361005, PR China

ARTICLE INFO

Article history:
Received 10 May 2019
Received in revised form 26 July 2019
Accepted 27 August 2019
Available online 20 September 2019

Keywords:
Flexible
Carbon nanotubes
Capacitance
Nanofiber
Pressure sensor

ABSTRACT

Flexible pressure sensors have been increasingly recognized over the past several decades, but there is still a challenge to fabricate them with a superb sensitivity and large sensing range. In this paper, a flexible capacitive pressure sensor based on the electrospun polyvinylidene fluoride (PVDF) nanofiber membrane with carbon nanotubes (CNTs) was developed to measure the pressure. The electrospinning CNT-PVDF nanofiber membrane can overcomes the limitations of the traditional solution-dip-coating for adhering conductive materials to the porous surface. The microstructure and characterization of the CNT-PVDF nanofiber membrane were analyzed by SEM, AFM and FTIR. By increasing the permittivity and decreasing the Young's modulus of the CNT-PVDF dielectric layer, the capacitive sensor exhibits high sensitivity (~0.99/kPa), fast response (~29 ms) and excellent cyclic loading/unloading stability (>1000 cycles). Moreover, experiments were also conducted to investigate influence of the thickness and bending radius of the sensor as well as temperature and humidity of the environment. In addition, a 3 × 3 sensor network attached on the hand was used to measure the spatial distribution and magnitude of tactile pressure. The proposed sensor has great potential for application in soft robotics and electronic skin.

1. Introduction

Flexible electronic sensors have been getting more and more attentions for potential applications on portable and foldable devices [1–3]. Among the various types of electronic sensors, pressure sensors are one of the most interested elements due to their potentials for various applications including folding wing airplane [1,4], soft robotics [5,6], electronic skins [7,8] and biological sensing [9,10]. In general, the sensing mechanisms of pressure sensor can typically be classified into four categories: transistor [11,12], piezoelectricity [13,14], piezoresistance [15–17] and capacitance [18–20]. Although the piezoelectric sensors with high sensitivity and high stability were widely used in many fields, they cannot be used to measure the static pressure, and their application in pressure sensor is limited [21]. Many works have been done on piezoresistive sensor because of low cost and the simple structure. To improve their sensitivity, the porous materials (porous elastomers [22], electrospun nanofiber membrane [23], hetero contact structure [24] *etc.*) have been used for increasing the deformation of the piezoresistive sensors. However, the sensitivity was still low. The high contact resistance between conductive materials may critically restrict the application of the sensors.

Owing to the high stability, low power consumption and simple construction, the capacitive pressure sensors had been widely applied [25–27]. Nevertheless, their sensitivity was low. To improve the sensitivity of the capacitive sensor, the conductive fillers (Carbon nanotubes [28], Graphene [29], Metal nanowire [30] *etc.*) had been added into the elastomer to increase the dielectric constant change of the composite dielectric layer when external pressure was applied on it. However, the sensitivity was still low. After that, some structures (pyramid structure [31], micro-pillar structure [32] *etc.*) had been used to improve the sensitivity of the capacitive sensor. However, the sensitivity would decrease rapidly as the applied pressure increased. In addition, porous elastomers with low Young's modulus had been used for the dielectric layer of the capacitive sensors [33,34]. Comparing to the non-porous elastomer dielectric layer, the porous elastomer can be compressed easily, which can improve the sensitivity of the sensor. Recently, ionic hydrogel with high ionic conductivity and outstanding mechanical properties had been applied on the dielectric layer of capacitive sensor, which can form electrical double layer capacitors in the surface of the electrode [35–37]. However, the hydrogel without the elastomeric coating was highly susceptible to dehydration, which was directly related to the sensor life.

* Corresponding author.
E-mail address: xinlinqing@xmu.edu.cn (X. Qing).
[1] These authors contributed equality to this work.

https://doi.org/10.1016/j.sna.2019.111579
0924-4247/

Electrospinning is a straightforward, efficient and scalable technique to fabricate the porous nanofiber membrane [38]. Because of the low Young's modulus of the fibrous structure, a large compressed deformation can be achieved with a small external pressure applied on it. Carbon nanotubes (CNTs) with a high aspect ratio have been widely used for the preparation of pressure sensors due to their high electrical conductivity and excellent mechanical properties. In this paper, a highly sensitive flexible capacitive pressure sensor based on the electrospun polyvinylidene fluoride (PVDF) nanofiber membrane with CNTs was developed. This sensor contains a flexible 3D composite nanofiber membrane and is coated with two indium tin oxide polyethylene terephthalate (ITO-PET) films on the top and bottom. This electrospun nanofiber membrane can not only overcome the disadvantage of high Young's modulus elastomer with conductive fillers in capacitive sensors, but also avoid the high contact resistance and non-uniform distribution of conductive filters of piezoresistive sensors. After describing the response mechanism, the functionality of the sensors was validated with different thickness of sensing membrane as well as carbon nanotubes with different additions. In addition, the effects of temperature and humidity on the performance of sensor were also investigated.

2. Experiment

2.1. Design of the sensor

The composite nanofiber membrane was fabricated using electrospinning method. A PVDF (Mw∼1,000,000 g/mol) solution was produced by dissolving the PVDF powder in the organic solvent and stirring continuously at room temperature for 10 h. The organic solvent contains acetone and N, N-Dimethylformamide with the weight ratio of 2:3. Then, carbon nanotubes were added to different solutions with weight rations of 0.03, 0.05, 0.1 and 0.2 wt% of PVDF. Note that, since the mixed solution was used to fabricate the dielectric material of a capacitive sensor, the amount of the CNT additions were far from the percolation threshold concentration of the CNT in the PVDF. In order to make sure the CNTs could disperse uniformly in the solutions, the mixed solutions were stirred by magnetic stirring for 5 h first, then dispersed by ultrasonic for 2 h. The solutions were then deposited nanofiber using electrospinning. The CNTs with special physicochemical properties could be incorporated to form composite nanofibers. The feed rate was 0.2 ml/h, the voltage was 15 KV and the distance between the substrate and syringe was 15 cm. The formation of the composite nanofiber was attributed to phase separation of the PVDF and the CNTs during solvent evaporation. The fabrication process of the CNT-PVDF composite nanofiber and its schematic diagram were shown in Fig. 1(a) and (b). It be seen from the electrospun progress that, the color of the nanofibers on the collect board changes gradually from white to black with the increase of CNT addition. There were two goals the CNT mixed nanofibers can achieve: (1) improving the sensitivity of the sensor by increasing the dielectric constant of the nanofibers; (2) improving the sensing range of the sensor by increasing of Young's modulus of nanofibers. The composite nanofiber membrane was heated at 200 ° for 2 h to form many mesoscopic joints of nanofibers with enhanced mechanical robustness and then peeled off from the substrate finally. Note that our composite nanofiber membrane is very flexible and elastic so that it may be used for other flexible device applications.

A single sensor and a sensor array based on the CNT-PVDF composite nanofiber membrane as dielectric layer. For the single sensor, two pieces of indium tin oxide polyethylene terephthalate (ITO-PET, 6Ω/□) films connected with cooper wires by conductive epoxy were fixed on the top and bottom surface of the composite nanofiber membrane as electrodes to record the capacitance variation under external pressure. The schematic diagram and the actual diagram of the single sensor were shown in Fig. 1(c). The scanning electron microscope (SEM, SUPRA 55) images of the composite nanofiber membranes with different ratios of CNT additive were shown in Fig. 1(d)–(g). From the microstructure of the nanofiber, the as-spun CNT-PVDF composite nanofibers have a randomly oriented structure. The diameter of the nanofibers decreases first and then increases with an increasing of the CNT addition. One of the reason is that during the electrospinning processes, the flow rate is fixed and the PVDF solution will reduce with the increase of CNT addition, which results in a decrease of diameter of the nanofibers. In addition, the conductivity will increase with the increase of CNTs addition. Besides, the electrostatic force between the collector and the syringe spinneret will increase, therefore the nanofibers will be pulled thinner and longer. However, with the increase of CNTs addition, the CNTs prefer to agglomerate due to the strong van deer waals force. And thus, the diameter of the nanofiber will increase. The as-spun nanofibers with low content of CNT addition (<0.05%) had a smooth surface and a straight shape, the CNTs integrated in the nanofibers or the aggregation of the CNTs had not been found here. A small amount of CNTs aggregation can be seen in the microstructure with 0.1 wt% CNT addition of PVDF. When the CNT addition is up to 0.2 wt% of PVDF, many CNT aggregations can be seen in the microstructure. In addition, in order to prove that the CNTs were embedded in the nanofibers, some cross section images of the nanofibers with 0.05 wt% CNTs addition of PVDF was conducted by the SEM. As shown in Fig. 1(h), the microcracks and the CNTs disperse uniformly in the nanofibers. For the flexible sensor array, line patterns of the ITO were prepared on two PET substrates. The two ITO-PET electrodes were assembled such that the directions of the ITO electrodes were perpendicular to each other. The width of each ITO electrode and the distance between two adjacent ITO electrodes were all 5 mm.

2.2. Sensing principle

The schematic of the proposed flexible capacitive sensor based on the CNT-PVDF composite nanofiber membrane was shown in Fig. 2. In the composite CNT-PVDF nanofiber, the interfacial polarization in the electric field is an important factor to improve the permittivity. Under external pressure, the distance between two electrodes decrease (from d to d'), the electric-field strength between two electrodes at a given potential is increase (E = U/d). The interfacial polarization in the increased electric field will become sharper and the permittivity will further increase. Moreover, the denser distribution of the CNTs (from a to a') caused by the compression of the CNT-PVDF membrane, can also contribute to the increasing permittivity of the CNT-PVDF membrane [39]. Therefore, the capacitance of the sensor will increase rapidly when the external pressure is applied on the sensor. The detailed theory analyses are described as follows:

Based on the percolation theory [30], the permittivityof the composite nanofiber can be expressed as:

$$\varepsilon_c = \frac{\varepsilon_p}{|\alpha - \alpha_p|^m} \quad (1)$$

From the equation, it is obvious that the permittivity of the materials cane significantly improved by adding a small amount CNT near the percolation threshold. Where ε_c and ε_p are the permittivity of the composite nanofiber and the PVDF, respectively. a_p is the percolation threshold concentration of CNT in the PVDF. a is the real amount of the CNT addition. Generally, the value of a is smaller than that of a_p in this work. The parameter m denotes the scaling constant related to the material properties.

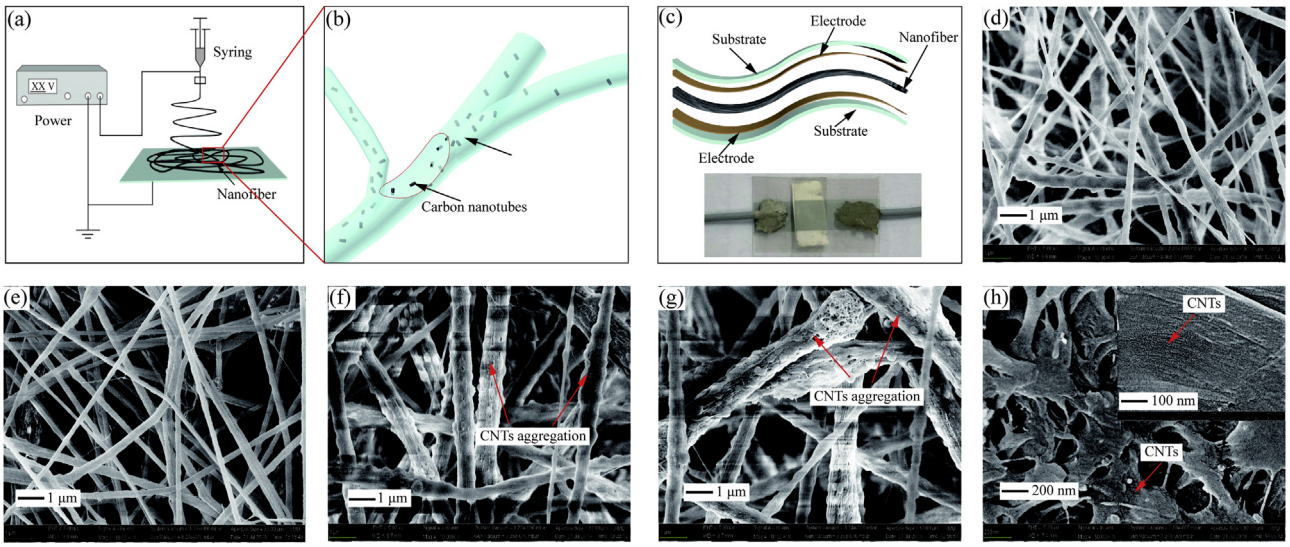

Fig. 1. Flexible capacitive pressure sensor: (a) Schematic of the fabrication of the composite nanofiber. (b) Schematic diagram of the composite nanofiber. (c) Diagram of the sensor. (d)–(h) The microstructures of the composite nanofiber membrane with 0.03, 0.05, 0.1, 0.2 wt% carbon nanotube additions, respectivity.

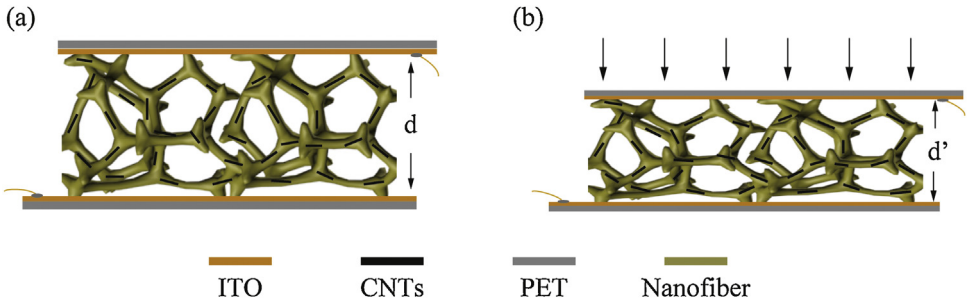

Fig. 2. Sensing principle of the flexible capacitive pressure sensor: (a) No external pressure applied on the sensor. (b) Pressure applied on the sensor.

According to the theory of binary systems of continuous medium and the uniform dispersoid [39], the permittivity of the composite nanofiber can be expressed as:

$$\varepsilon = \varepsilon_c[1 + \frac{nq(\varepsilon_a - \varepsilon_c)}{n\varepsilon_c + (\varepsilon_a - \varepsilon_c)(1-q)}] \quad (2)$$

Where ε is the permittivity of the porous composite nanofiber membrane without external pressure applied on it. q_0 is the volume fraction of pores. ε_a and ε_c are the permittivities of the air and the composite nanofiber, respectively. Note that, since the q_0 of the porous membrane is changeable under the external pressure (when the external pressure is applied on porous composite nanofiber membrane, the membrane will be compressed and the air will be exhausted.), the ε of the membrane varies with the external pressure.

The capacitance of the capacitive sensor is calculated by the following equation:

$$C = \frac{\varepsilon A}{d} \quad (3)$$

Where ε is the permittivity of the porous composite nanofiber membrane. A is the electrode-dielectric interfacial area, d is the distance between the top and the bottom electrodes.

From Eqs. (1) to (3), the relation between the external pressure and the capacitance of the sensor can be described as:

$$C = \varepsilon_a\varepsilon_c\frac{AE}{Ed-\sigma}[1 + \frac{n(Edq_0 - Ed\upsilon^2 - \sigma\upsilon^2)(\varepsilon_a - \varepsilon_c)}{Edn\varepsilon_c + (\varepsilon_a - \varepsilon_c)(Ed - Edq_0 - Ed\upsilon^2 + \sigma\upsilon^2)}] \quad (4)$$

Where E and υ are the Young's modulus and Poisson's ratio of the nanofiber membrane, respectively. Other symbols are the same as those in the previous Equations.

According to the theory analyzed above, the sensitivity of the sensor will be greatly enhanced and the detectable range for pressure will became significantly wide by improving the deformability and elasticity of such a composite nanofiber dielectric layer with micro-pores and CNTs integrated. Moreover, the sensitivity and sensing range of the sensor can be adjusted by different kinds of porosity and CNTs additions in the dielectric layer.

3. Results and discussion

3.1. AFM and FTIR analysis of CNT-PVDF composite nanofibers

In order to investigate the influence of CNT additions to the surface structure of nanofibers, atomic force microscope (AFM, Cypher S) analysis was applied to obtain the information about the surface structures of the CNT-PVDF composite nanofibers. AFM can provide the measurement information about the surface roughness of polymers. As shown in Fig. 3(a)–(e), the roughness of the nanofibers decreases first and then increases with the increase of the CNT addition. The surface roughness of the composite nanofiber membrane with 0, 0.03%, 0.05%, 0.1% and 0.2% CNT additions are 1.40 μm, 0.85 μm, 0.60 μm, 0.85 μm and 1.60 μm, respectively. The diameter and the roughness of the nanofibers membrane will decrease when the amount of the CNT addition is less than 0.05 wt% of PVDF. When the content of CNT addition increases to 0.2 wt % of PVDF, the roughness

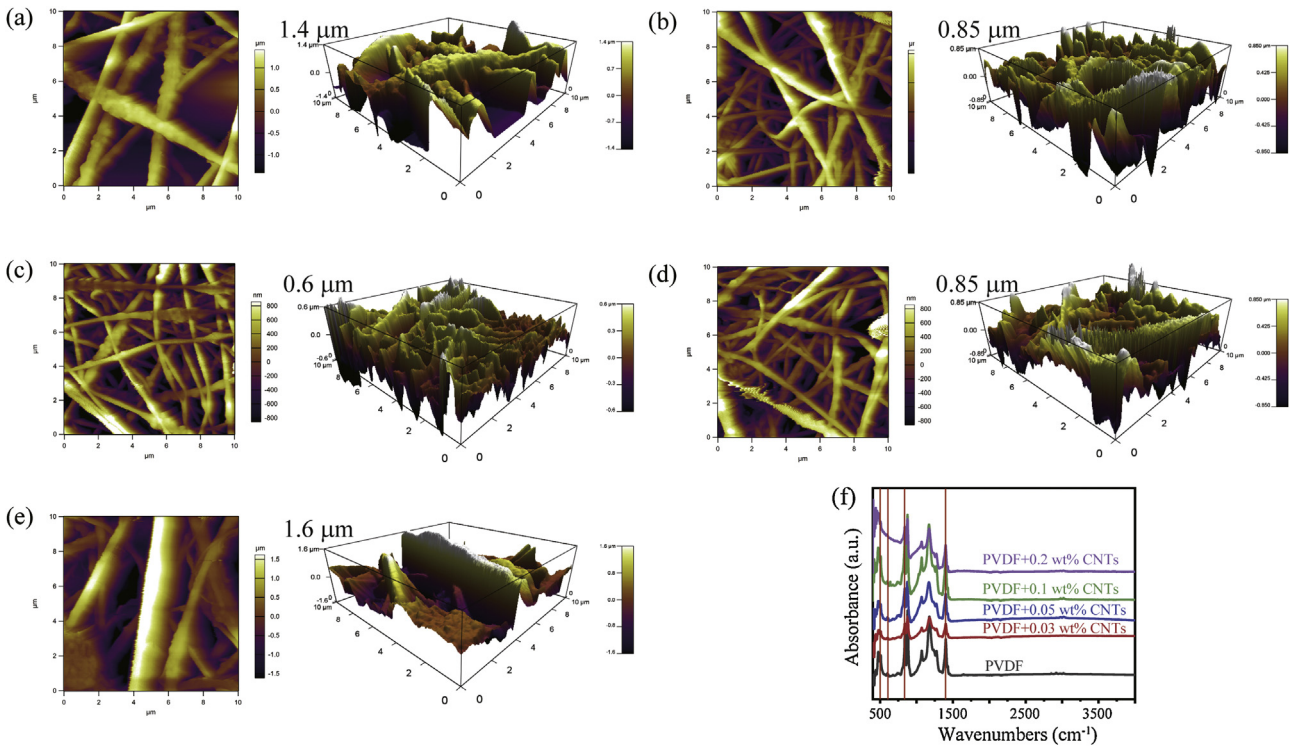

Fig. 3. AFM images and FTIR spectra of the composites nanofiber samples: (a)–(e), The AFM images of the composites nanofiber without 0, 0.03, 0.05, 0.1, 0.2 wt% CNTs addition of PVDF, respectively. (f) The FTIR spectra of composites nanofiber with different CNTs addition.

and the diameter of nanofibers will increase due to the aggregation of CNT in the nanofibers.

Besides, fourier transform infrared spectrums (FTIR, Nicolet IS10) was used to determine the crystal structures of the nanofibers. The FTIR spectra were recorded within the range of 400 cm^{-1} to 4000 cm^{-1} at a spectral of 2.2 cm^{-1}. As shown in Fig. 3(f), no other new bands appeared after CNTs were embedded into the nanofibers, and the characteristic of β phase was observed at 510 cm^{-1}, 598 cm^{-1}, 845 cm^{-1} and 1400 cm^{-1}, respectively. According to the results, the CNTs dispersed in the nanofibers didn't form a new phase.

3.2. The initial capacitance and density analysis of the CNT-PVDF composite nanofibers

As theory analyzed above, with the addition of CNT, the relative permittivity will gradually increase when the CNT concentration is below the percolation threshold. The relative permittivity of the CNT-PVDF composite nanofiber membrane has been experimentally investigated. Without CNT addition the permittivity of neat PVDF nanofiber membrane is 3.8; but after adding 0.03 wt% CNT, the permittivity is increased to 8.3. When the CNT addition is increased to 0.05 wt%, 0.1 wt% and 0.2 wt%, the permittivity is increased to 12.6, 15.2 and 17.6, respectively. In addition, the initial capacitance of the capacitive sensor with different CNT additions has been measured, as shown in Fig. 4(a). It is obvious that the capacitive increases with the increase of CNT addition. The initial capacitance of the capacitive sensor without CNT addition is 12.54 pF. The initial capacitance increases from 27.32 pF to 57.73 pF when the CNT addition increases from 0.03 wt% to 0.2 wt%.

In addition, the density of the CNT-PVDF composite nanofiber membrane has been measured. As shown in Fig. 4(b), the density of the nanofiber increases from 0.90 g/cm^3 to 1.29 g/cm^3 with the CNTs addition increase from 0 to 0.2 wt%.

3.3. Relationship between the pressure and change of the capacitance

The experimental setup is shown in Fig. 5(a). During the experiment, the load was supplied by a force gauge, and the capacitance of the sensor was recorded by an impedance analyzer (WK 6500B) with a voltage of 1 V at a frequency of 300 Hz. Fig. 5(b) shows the relationship between the actual pressure applied on the sensor and the capacitance of the sensor fabricated by pure PVDF nanofiber membrane. The sensing area of the sensor was 5 mm × 5 mm and the thickness of the composite nanofiber membrane was given at 20.1 μm. As the pressure was applied on the sensor, the capacitance of the sensor was measured by the impedance analyzer in real-time. The sensitivity (S) of the capacitive sensor can be defined as the slope rate of the curve ($S=\delta(\triangle C/C_0)/\delta P$). Where P denotes the external pressure applied on the sensor. The $\triangle C$ and C_0 denote the capacitance change and the initial capacitance of the sensor, respectively. It is clear that the change of the capacitance depends on the pressure. The sensitivity was 0.09/kPa when the pressure was below 0.9 kPa, and it would reduce to 0.02/kPa when the pressure was increased form 0.9 kPa to 7.0 kPa. Fig. 5(c) illustrates the capacitance change of the developed sensor with different levels of pressure applied on, given the CNT additions varies from 0.03 to 0.2 wt% of PVDF. The thickness of the composite nanofiber membrane was 20.1 μm and the dimension of the sensing area was the same as the sensor fabricated by pure PVDF nanofiber membrane. Besides, once the pressure was applied on the sensor, the CNT-PVDF composite nanofiber dielectric layer was compressed, then the distance between two electrodes and the CNTs would decrease, the capacitance would increase immediately. According to the experimental results, the sensitivity of the sensor would increase first and then decreases before the CNT addition increases to 0.2 wt% of PVDF. These results match well with the AFM results mentioned before. The composite nanofiber membrane with a composition of 0.05 wt% CNT addition had the highest aver-

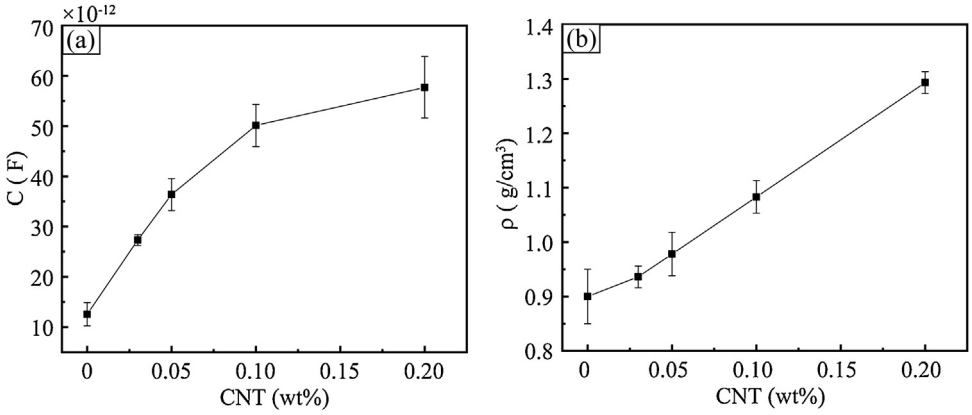

Fig. 4. The characteristic of the nanofiber fibers: (a) The initial capacitance of the sensor with different CNT additions. (b) The density of the cpmposite nanofiber with different CNT additions.

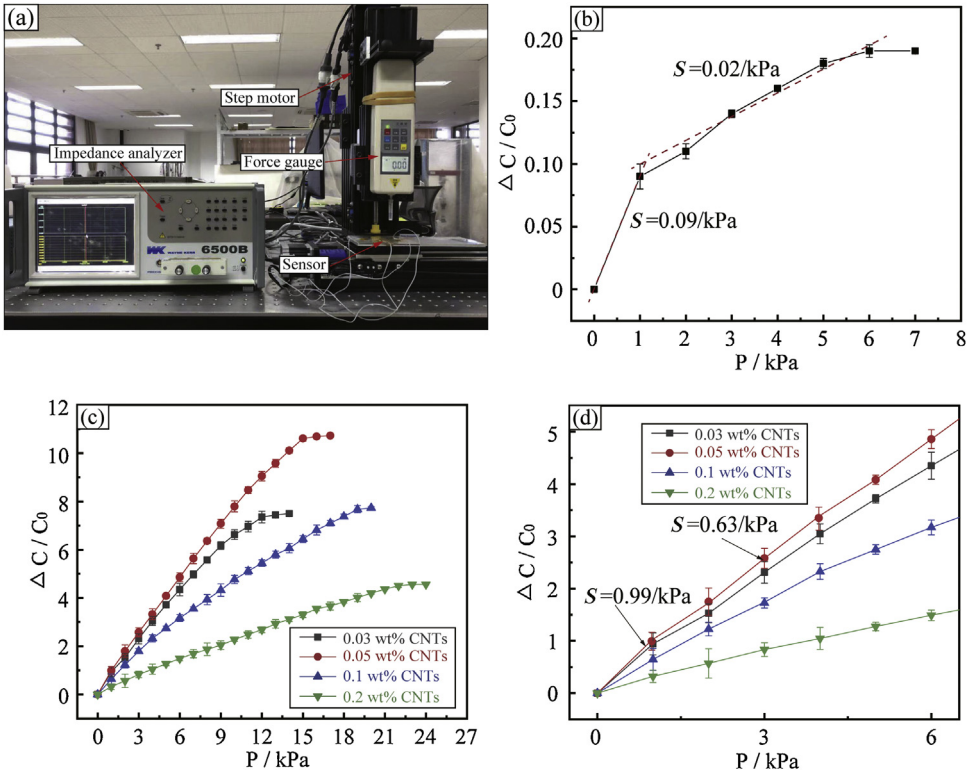

Fig. 5. Characterization of the pressure sensing performance of the flexible capacitive sensor: (a) Experimental systems for applying pressure and measuring capacitance. (b) The relationship between external pressure and capatitance change of the sensor fabricated by pure PVDF nanofiber membrane. (c)The relative change in capacitance of the sensor with different weight ratio CNTs addition under pressure applied. (d) The low pressure area of (c).

Table 1
Comparison of the sensing properties of pressure sensorswith different Carbon Nanotubes addition and some previous reported pressure sensors.

Types	Dielectric layer	Sensitivity
Silicon-based	Air [26]	0.06/kPa (0–0.03 kPa)
Elastic material-based	PDMS [30]	0.0014/kPa (0–10 kPa)
	CNT/PDMS [30]	0.0072/kPa (0–10 kPa)
	Pyramid PDMS [31]	0.55/kPa (0–2 kPa)
	Porous PDMS [33]	0.26/kPa (0–0.02 kPa)
Microfluidic-based	Hydrogel [36]	0.02/kPa (0–0.2 kPa)
CNT-PVDF Nanofiber-based	Nanofiber(0 % CNT) (this work)	0.09/kPa (0–0.9 kPa) 0.02/kPa (0.9–8 kPa)
	Nanofiber(0.03% CNT) (this work)	0.94/kPa (0–0.8 kPa) 0.58/kPa (0.8–12.2 kPa)
	Nanofiber(0.05% CNT) (this work)	0.99/kPa (0–1.2 kPa) 0.63/kPa (1.2–15.0 kPa)
	Nanofiber(0.1% CNT) (this work)	0.64/kPa (0–1.1 kPa) 0.41/kPa (1.1–19.4 kPa)
	Nanofiber(0.2% CNT) (this work)	0.32/kPa (0–1.6 kPa) 0.21/kPa (1.6–22.1 kPa)

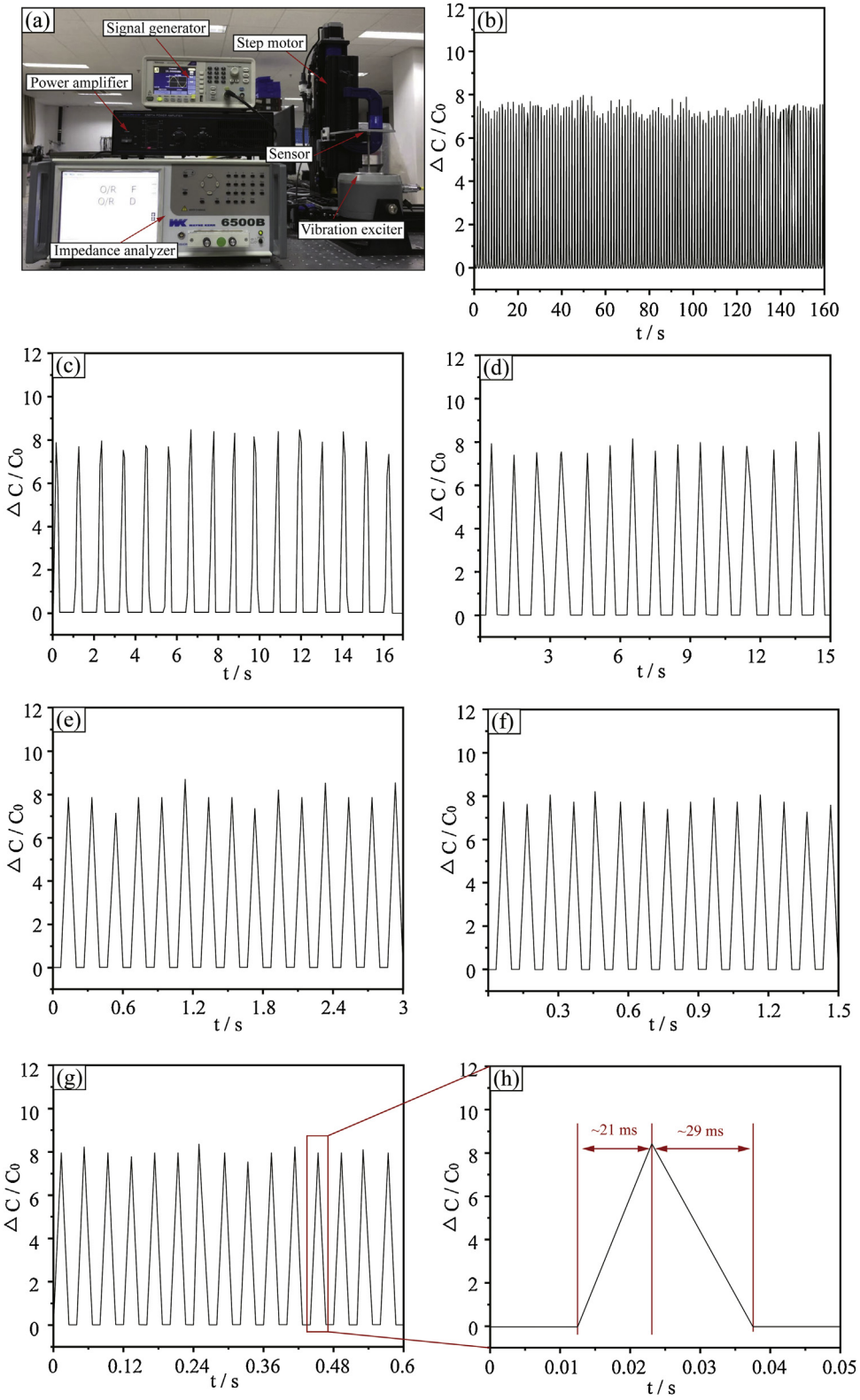

Fig. 6. Characterization of the pressure sensing performance of the flexible capacitive sensor: (a) Experimental systems for dynamic pressure applying and measuring capacitance. (b)–(g) The relationship of pressure and capacitance of the sensor compressed by a periodic pressure at 1, 3, 5, 10 and 25 Hz. (h) The enlarged view of a portion of the figure (g).

age sensitivity of 0.99/kPa when the pressure was below 1.2 kPa, and it would reduce to 0.63/kPa when the pressure was increased from 1.2 kPa to 15.0 kPa (Fig. 5(d)). The sensitivity and the sensing range of the sensors with different CNT additions as well as some similar capacitive sensor were shown in Table 1. Note that, when the pressure is continuously increased, the sensitivity decreases due to the increased Young's modulus of the CNT-PVDF composite nanofibers. There are two relevant factors: (1) the "spring con-

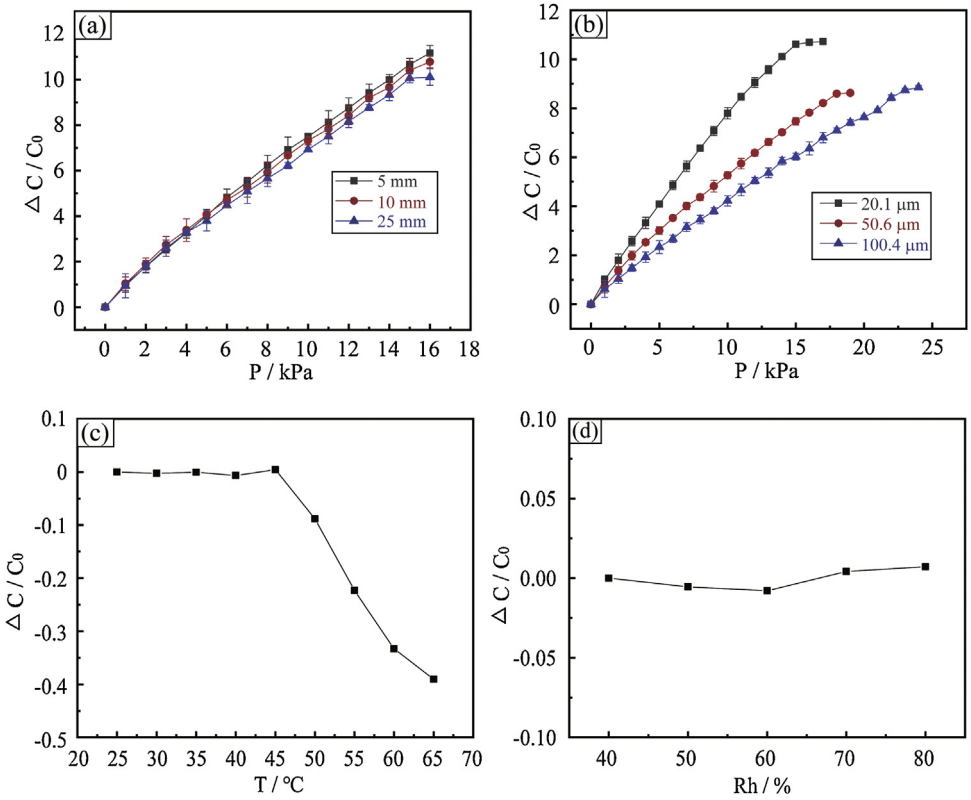

Fig. 7. Influence of some factors on the sensing performance: (a) Relationship of the change in capacitance of the sensor attached on circular tubes with radius at 5, 10, 25 mm. (b) Different thickness of the nanofiber membrane, 20.1, 50.6, 100.4 μm. (c) Capacitance change with frequency at temperature range from 25 ° to 70 °. (d) Capacitance follows the frequency at humidity range from 40% to 80%.

stant" of nanofibers is increased under press, (2) more and more nanofibers get into contact with the electrodes under press.

In summary, comparing to the capacitive sensor fabricated by pure PVDF nanofiber membrane, the sensitivity and the sensing range of the capacitive sensor fabricated by composite PVDF nanofiber with CNT addition were greatly enhanced. The sensitivity of the sensor will increase first and then decrease with the increase of the CNT addition. Experimental results show that, the sensitivity of the sensor with 0.05 wt% CNT addition of PVDF is the highest, and it decreases with further increase of the CNT addition. The reason is that the aggregation of CNT in CNT-PVDF composite nanofibers with high CNT addition becomes more severe. Therefore, the developed sensor with 0.05% CNTs is used for the following experiments.

A dynamic pressure provided by a vibration exciter at 1, 3, 5 and 10 Hz, was applied on the sensor with 0.05 wt% CNT contents of PVDF. The thickness of the CNT-PVDF composite nanofiber dielectric layer is 20.1 μm. The dynamic experimental setup was shown in Fig. 6(a), the capacitance of the sensor was recorded by the impedance analyzer. To evaluate the reversibility and the reproducibility of the sensor, the repetitional cycles of tests were conducted by applying and releasing the pressure of 10 kPa for 1000 times. The relevant changes in capacitance of the sensor with 1000 cycles applying in 1 Hz were shown in Fig. 6(b). The random consecutive fifteen cycles in the 1000 cycles of the capacitance curves with 1, 3, 5, 10 and 25 Hz were shown in Fig. 6(c)–(g), the capacitance curves were stable and matched well with the external pressure. The response and relaxation time of the sensor were 21 ms and 29 ms, which can be extracted from the upstroke response of the device readout signal in Fig. 6(h). Because of the viscoelasticity of the PVDF, the relation time is longer than the response time. Moreover, the capacitance can come back to the original value when the pressure was released to zero. Overall, the sensor is able to respond well to both static and dynamic applied pressure. Note that this sensor cannot measure the highly frequent pressure, it may due to the viscoelasticity of the CNT-PVDF composite nanofiber.

3.4. Effect of the bending radius of the sensor

In real applications, the flexible sensor may be attached on many complex structures to measure the surface pressures. Therefore, it is important to study the influence of different bending radiuses on the sensing performance of sensors. The sensors equipped with composite nanofiber membrane, which has 20.1 μm thickness and 0.05 wt% CNT addition were attached on the cylinder with radiuses of 5 mm, 10 mm and 25 mm, respectively. In order to avoid bending the bottom electrode only, the top electrode was attached on the cylinders by a polyimide type. As shown in Fig. 7(a), the capacitance changes of the sensors attached on the cylinders with different radiuses can be negligible. It can be inferred that the sensors are insensitive to the bending radius and are fitted to measure the pressure applied on complex structures.

3.5. Effect of the thickness of the dielectric layer

As mentioned before, the sensitivity and the sensing range can be adjusted by changing the thickness of the dielectric layer. In order to meet the practical engineering application, it is important to investigate the influence of thickness on both sensing range and sensitivity of the developed sensor. Fig. 7(b) shows the relation between the change of the capacitance and the actual pressure applied on the sensors with different thicknesses of the composite nanofiber dielectric layer varying from 20.1 μm to 100.4 μm. It is obvious that the sensitivity will decrease from 0.99/kpa to 0.53/kPa, and the sensing range will increase from 15 kPa to 23 kPa with the thickness of dielectric layer increase from 20.1 μm to 100.4 μm.

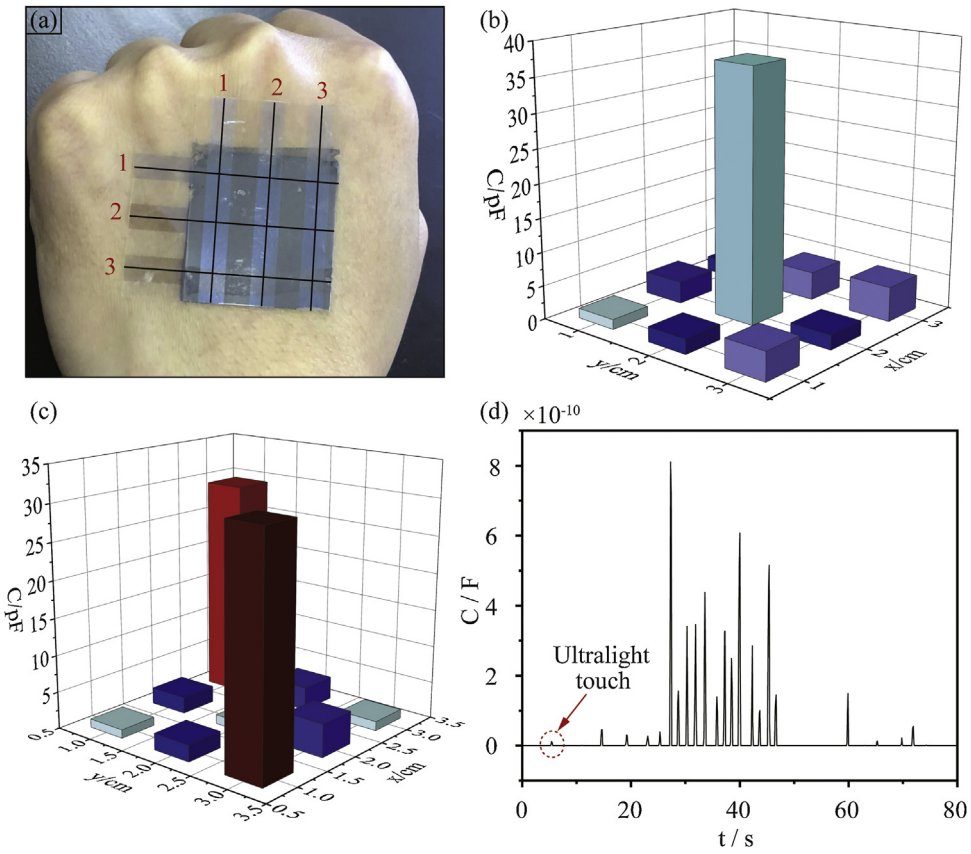

Fig. 8. Wearable sensor for finger pressure sensing: (a) The diagram of sensor network attached on the hand (b), (c) The measured capacitance change when a single and double pressure applied on the sensor network. (d) Plots showing the relative changes in capacitance of the sensor when it was subjected to dynamic pressing and releasing cycles.

According to these results, we can choose the appropriate thickness of the dielectric layer to meet different measurement requirements.

3.6. Effect of the temperature and the humidity

In real applications, the sensor is generally working in a very complex environment, where the humidity and the temperature often vary in time. As shown in Fig. 7(c), the capacitances of the sensor were measured at the temperature range between 25 ° and 65 °. It is clear that the capacitances were decrease slowly under the temperature between 25 ° and 45 °, but decreases fast at 50 °. Within the temperature range from 25 ° to 45 °, the temperature sensitivity is less than $8*10^{-3}$/°, which means that the capacitance can be considered as stable in this temperature range. With continuously increasing the temperature, the capacitance of the sensor decreases fast, it may cause by the phase transform of the CNT-PVDF composite nanofibers. The temperature sensitivity is about 0.02/° in the temperature range from 45 to 65 /°.

Meanwhile, the sensing performance of the sensor at different humidity level has been investigated. As shown in Fig. 7(d), the humidity sensitivity of the sensor is quite small at different humidity level ranging from 40% to 80%, which indicates that the capacitance of the sensor is stable at the humidity. This is because the CNT-PVDF composite nanofiber dielectric layer is stable at different humidity levels, which can be proved by maintaining the same microstructures before and after washing.

3.7. Application for electronic skin

An essential function of electronic skin is to sense haptic perception, such as surface pressure, perception and lateral motion. To demonstrate the high sensitivity and flexibility of the proposed sensor, a 3 × 3 sensor network was attached on the skin to measure the surface pressure. As shown in Fig. 8(a)–(c), the sensor network was attached on the surface of the hand to record the surface pressure. The sensor network was subjected to a single, double and cyclical tactile pressure, and the capacitance was measured by the impedance analyzer in real time. As shown in Fig. 8(d), the sensor network was sensitive to the tactile pressure, when the pressure was applied on the sensor, the capacitance increase immediately, and the capacitance variation was positively correlated with the pressure applied on the sensor. The capacitance of the sensor returned to its initial state rapidly when pressure was released. Importantly, by repeating the same pressure for numerous times, we also demonstrated the stability of the sensor. According to these results, the sensor has the potential value in the application of soft robotics and electronic skin.

4. Conclusions

A highly sensitive flexible capacitive sensor based on the electrospun CNT-PVDF composite nanofiber membrane was developed, and its pressure sensing properties show that a 0.05 wt% CNT addition of the PVDF and the thickness of 20.1 μm was the optimal process. Based on the experimental results, the following marks can be made:

- The sensor responds well under both static and dynamic pressure (~29 ms) with high sensitivity, good linearity and nice repeatability;
- This sensor can provide a high sensitivity up to 0.99/kPa;

- The sensitivity and the sensing range of the sensor can be adjusted by modulating the ratios of the CNTs and the thickness of the dielectric layer;
- The capacitance of the sensor with selected materials is not sensitive to the humidity.

Overall, the developed innovative sensor has a significant potential for the low cost and reliable electronic skin, soft robots, aerodynamic pressure measurement and other important fields.

Acknowledgements

The authors are grateful for the support by the National Natural Science Foundation of China (No. 11772279), National Key Research and Development Program of China (No. 2016YFF0203002) and the Fundamental Research Funds for the Central Universities (No. 20720180120).

References

[1] C. Kokkinos, M. Angelopoulou, A. Economou, M. Prodromidis, A. Florou, W. Haasnoot, et al., Lab-on-a-membrane foldable devices for duplex drop-volume electrochemical biosensing using quantum dot tags, Anal. Chem. 88 (2016) 6897–6904.
[2] Y. Sun, R.B. Sills, X. Hu, Z.W. Seh, X. Xiao, H. Xu, et al., A bamboo-inspired nanostructure design for flexible, foldable, and twistable energy storage devices, Nano Lett. 15 (2015) 3899–3906.
[3] J. Choi, A.W. Gani, D.J. Bechstein, J.-R. Lee, P.J. Utz, S.X. Wang, Portable, one-step, and rapid GMR biosensor platform with smartphone interface, Biosens. Bioelectron. 85 (2016) 1–7.
[4] A. Castrichini, V. Hodigere Siddaramaiah, D. Calderon, J.E. Cooper, T. Wilson, Y. Lemmens, Nonlinear folding wing tips for gust loads alleviation, J. Aircr. Spacecr. Technol. 53 (2016) 1391–1399.
[5] S.A. Morin, R.F. Shepherd, S.W. Kwok, A.A. Stokes, A. Nemiroski, G.M. Whitesides, Camouflage and display for soft machines, Science 337 (2012) 828–832.
[6] S.-H. Chiu, P.L. Urban, Robotics-assisted mass spectrometry assay platform enabled by open-source electronics, Biosens. Bioelectron. 64 (2015) 260–268.
[7] J. Kim, M. Lee, H.J. Shim, R. Ghaffari, H.R. Cho, D. Son, et al., Stretchable silicon nanoribbon electronics for skin prosthesis, Nat. Commun. 5 (2014) 5747.
[8] C. Wang, D. Hwang, Z. Yu, K. Takei, J. Park, T. Chen, et al., User-interactive electronic skin for instantaneous pressure visualization, Nat. Mater. 12 (2013) 899.
[9] S. Prakash, T. Chakrabarty, A.K. Singh, V.K. Shahi, Polymer thin films embedded with metal nanoparticles for electrochemical biosensors applications, Biosens. Bioelectron. 41 (2013) 43–53.
[10] J. Zou, M. Zhang, J. Huang, J. Bian, Y. Jie, M. Willander, et al., Coupled supercapacitor and triboelectric nanogenerator boost biomimetic pressure sensor, Adv. Energy Mater. 8 (2018), 1702671.
[11] S.H. Shin, S. Ji, S. Choi, K.H. Pyo, B. Wan An, J. Park, et al., Integrated arrays of air-dielectric graphene transistors as transparent active-matrix pressure sensors for wide pressure ranges, Nat. Commun. 8 (2017) 14950.
[12] S. Jang, E. Jee, D. Choi, W. Kim, J.S. Kim, V. Amoli, et al., Ultrasensitive, low-power oxide transistor-based mechanotransducer with microstructured, deformable ionic dielectrics, ACS Appl. Mater. Interfaces 10 (2018) 31472–31479.
[13] L. Wu, W. Yuan, N. Hu, Z. Wang, C. Chen, J. Qiu, et al., Improved piezoelectricity of PVDF-HFP/carbon black composite films, J. Phys. D Appl. Phys. 47 (2014), 135302.
[14] X. Li, E.C. Kan, A wireless low-range pressure sensor based on P(VDF-TrFE) piezoelectric resonance, Sens. Actuators A Phys. 163 (2010) 457–463.
[15] J. Park, Y. Lee, J. Hong, M. Ha, Y.-D. Jung, H. Lim, et al., Giant tunneling piezoresistance of composite elastomers with interlocked microdome arrays for ultrasensitive and multimodal electronic skins, ACS Nano 8 (2014) 4689–4697.
[16] W. Zhang, B. Yin, J. Wang, A. Mohamed, H. Jia, Ultrasensitive and wearable strain sensors based on natural rubber/graphene foam, J. Alloys. Compd. 785 (2019) 1001–1008.
[17] J. Li, S. Orrego, J. Pan, P. He, S.H. Kang, Ultrasensitive, flexible, and low-cost nanoporous piezoresistive composites for tactile pressure sensing, Nanoscale 11 (2019) 2779–2786.
[18] X. Yang, Y. Wang, X. Qing, A flexible capacitive pressure sensor based on ionic liquid, Sensors Basel (Basel) 18 (2018) 2395.
[19] Z. He, W. Chen, B. Liang, C. Liu, L. Yang, D. Lu, et al., Capacitive pressure sensor with high sensitivity and fast response to dynamic interaction based on graphene and porous nylon networks, ACS Appl. Mater. Interfaces 10 (2018) 12816–12823.
[20] H.-K. Kim, S. Lee, K.-S. Yun, Capacitive tactile sensor array for touch screen application, Sens. Actuators A 165 (2011) 2–7.
[21] L. Persano, C. Dagdeviren, Y. Su, Y. Zhang, S. Girardo, D. Pisignano, et al., High performance piezoelectric devices based on aligned arrays of nanofibers of poly(vinylidenefluoride-co-trifluoroethylene), Nat. Commun. 4 (2013) 1633.
[22] L. Zhao, F. Qiang, S. Dai, S. Shen, Y. Huang, N.-J. Huang, et al., Construction of sandwich-like porous structure of graphene-coated foam composites for ultrasensitive and flexible pressure sensor, Nanoscale (2019).
[23] L. Zhu, X. Zhou, Y. Liu, Q. Fu, Highly Sensitive, Ultrastretchable Strain Sensors Prepared by Pumping Hybrid Fillers of Carbon Nanotubes/Cellulose Nanocrystal into Electrospun Polyurethane Membranes, ACS Appl. Mater. Interfaces 11 (2019) 12968–12977.
[24] X. Liao, W. Song, X. Zhang, H. Zhan, Y. Liu, Y. Wang, et al., Hetero-contact microstructure to program discerning tactile interactions for virtual reality, Nano Energy (2019).
[25] J. Wang, R. Suzuki, M. Shao, F. Gillot, S. Shiratori, Capacitive pressure sensor with wide-range, bendable, and high sensitivity based on the bionic komochi konbu structure and Cu/Ni nanofiber network, ACS Appl. Mater. Interfaces 11 (2019) 11928–11935.
[26] S. Kohli, A. Saini, A.J. Pillai, Mems based capacitive pressure sensor simulation for healthcare and biomedical applications, Inter J Sci Eng Res 4 (2013) 1855–1862.
[27] D.P.J. Cotton, I.M. Graz, S.P. Lacour, A multifunctional capacitive sensor for stretchable electronic skins, IEEE Sens. J. 9 (2009) 2008–2009.
[28] L. Chen, J. Liu, X. Wang, B. Ji, X. Chen, B. Yang, Flexible capacitive hydrogel tactile sensor with adjustable measurement range using liquid crystal and carbon nanotubes composites, Ieee T Electron. Dev. 64 (2017) 1968–1972.
[29] O. Atalay, A. Atalay, J. Gafford, C. Walsh, A highly sensitive capacitive-based Soft pressure sensor based on a conductive fabric and a microporous dielectric layer, Adv. Mater. Technol. 3 (2018), 1700237.
[30] S.-Y. Liu, J.-G. Lu, H.-P.D. Shieh, Influence of Permittivity on the sensitivity of porous elastomer-based capacitive pressure sensors, IEEE Sens. J. (2018) 1870–1876.
[31] S.C. Mannsfeld, B.C. Tee, R.M. Stoltenberg, C.V. Chen, S. Barman, B.V. Muir, et al., Highly sensitive flexible pressure sensors with microstructured rubber dielectric layers, Nat. Mater. 9 (2010) 859–864.
[32] T. Li, H. Luo, L. Qin, X. Wang, Z. Xiong, H. Ding, et al., Flexible capacitive tactile sensor based on micropatterned dielectric layer, Small 12 (2016) 5042–5048.
[33] S. Chen, B. Zhuo, X. Guo, Large area one-step facile processing of microstructured elastomeric dielectric film for high sensitivity and durable sensing over wide pressure range, ACS Appl. Mat. Interfaces 8 (2016) 20364–20370.
[34] B.-Y. Lee, J. Kim, H. Kim, C. Kim, S.-D. Lee, Low-cost flexible pressure sensor based on dielectric elastomer film with micro-pores, Sens. Actuators A. 240 (2016) 103–109.
[35] B. Nie, R. Li, J. Cao, J.D. Brandt, T. Pan, Flexible transparent iontronic film for interfacial capacitive pressure sensing, Adv. Mater 27 (2015) 6055–6062.
[36] J.Y. Sun, C. Keplinger, G.M. Whitesides, Z. Suo, Ionic skin, Adv. Mater. 26 (2014) 7608–7614.
[37] X. Yang, Y. Wang, H. Sun, X. Qing, A flexible ionic liquid-polyurethane sponge capacitive pressure sensor, Sens. Actuators A. 285 (2019) 67–72.
[38] N. Bhardwaj, S.C. Kundu, Electrospinning: a fascinating fiber fabrication technique, Biotechnol. Adv. 28 (2010) 325–347.
[39] T. Yamada, T. Ueda, T. Kitayama, Piezoelectricity of a high-content lead zirconate titanate/polymer composite, J. Appl. Phys. 53 (1982) 4328–4332.

Biographies

Xiaofeng Yang, received his B.Sc. degree in 2013 from Jiangsu University of Science and Technology, Zhenjiang, China, the M.Sc. degree from Xiamen University, Xiamen, China, in 2016. Currently, he is a Ph.D. candidate in Xiamen University. His main research interests include advanced sensing technology.

Yishou Wang, received his B.Sc. and Ph. D. degrees from Dalian University of Technology, Dalian, China, in 2002 and 2008, respectively. Now, he is an associate professor in Xiamen University, Xiamen, China. His main research interests include structural health monitoring and advanced sensing technology.

Xinlin Qing received his M.Sc. degree in 1991 from Tianjin University, Tianjin, China, the Ph.D. degree from Tsinghua University, Beijing, China, in 1993. Currently he is a distinguished professor in Xiamen University, Xiamen, China. His main research interests include structural health monitoring and advanced sensing technology.